Supporting Information

Spin Dynamic of Tri-addition Endohedral Nitrogen Fullerene with Transversal Chemical Functionalization

Cong-Hui Wu, Yu-jin Wu, Jia-Yue Yuan, Zhi-Rong Wu, Qi Xiong, Li-Nan Zhou, Song Gao, Shen Zhou, Shang-Da Jiang

Supporting Information

Contents

SI 1: Mass Spectra for products 3 and 5

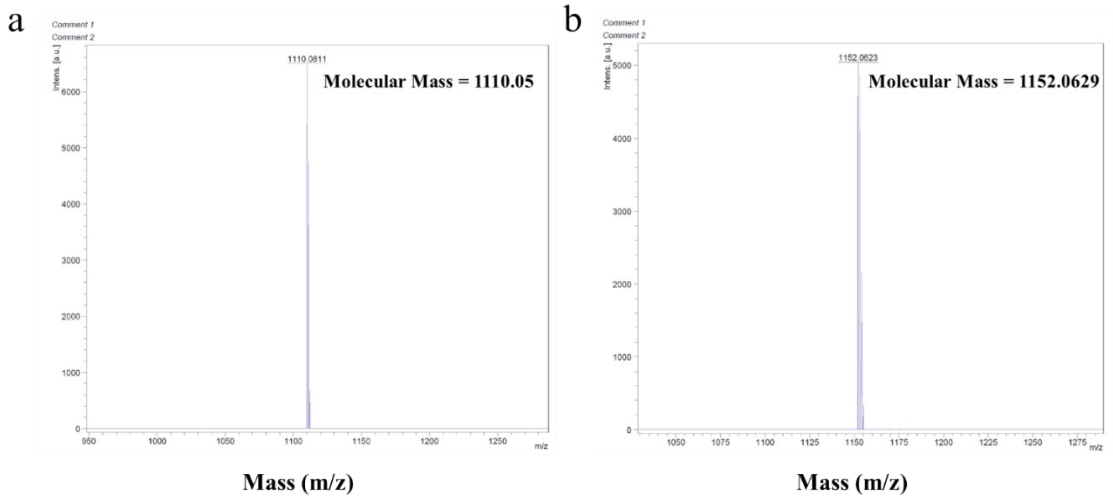

Figure S1 MALDI-TOF-MS of a) 3, b) 5 (Trans-2-[3-(4-tert-Butylphenyl)-2-methyl-2-propenylidene] malononitrile and negative mode)

SI 2: T_1 measurement of 3 and 5 powder at 3456 G

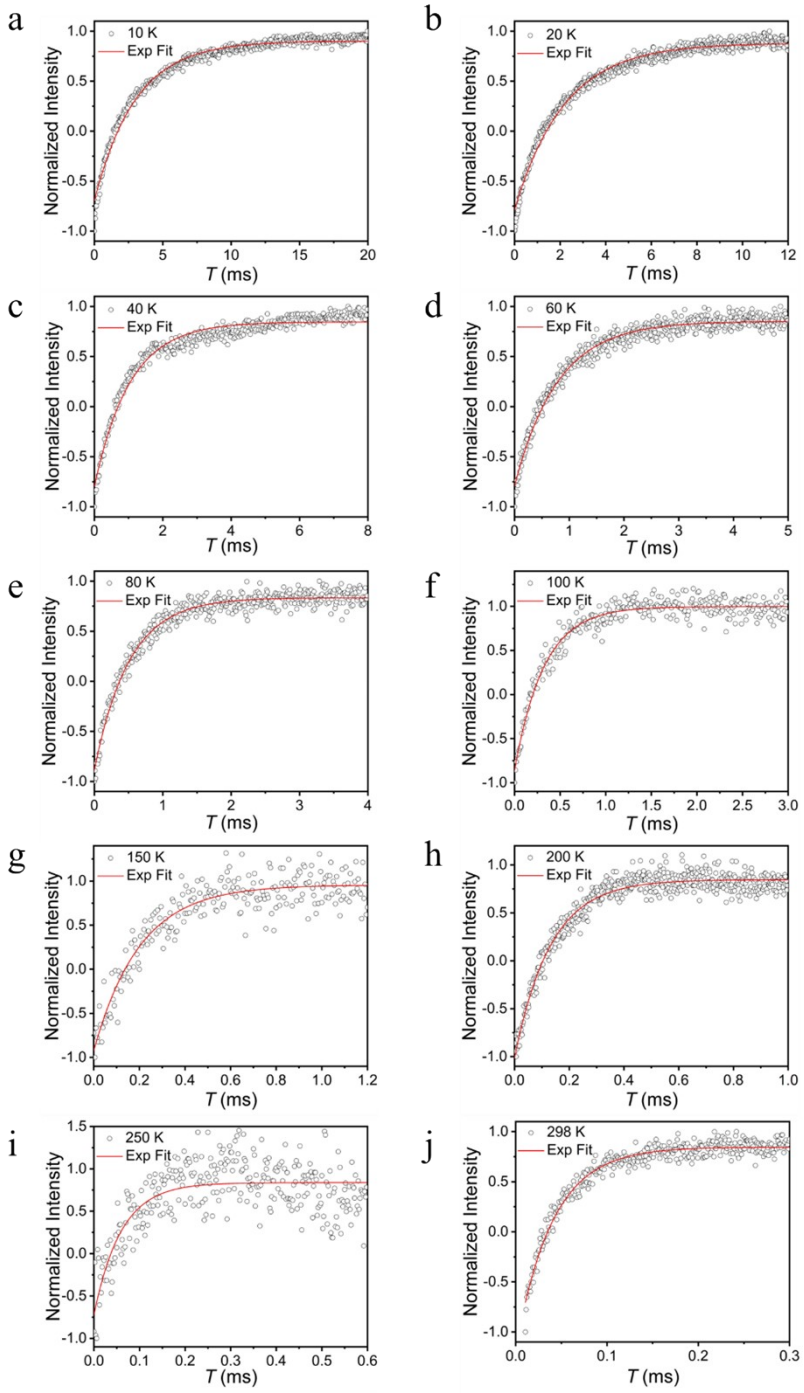

Figure S2 (a-j) T_1 data (black point) measured at different temperatures at 3456 G and individual exponential fitting curves (red line) for 3 powder. At higher temperatures, the signal becomes weaker, necessitating more repetitions to obtain reliable results. The shots per point for Figure S2 h and i (200 and 250 K) are twice as many as those used for Figure S2 a–g (from 10 to 150 K), and the shots per point for Figure S2 j (298 K) are four times greater than those used for Figure S2 a–g.

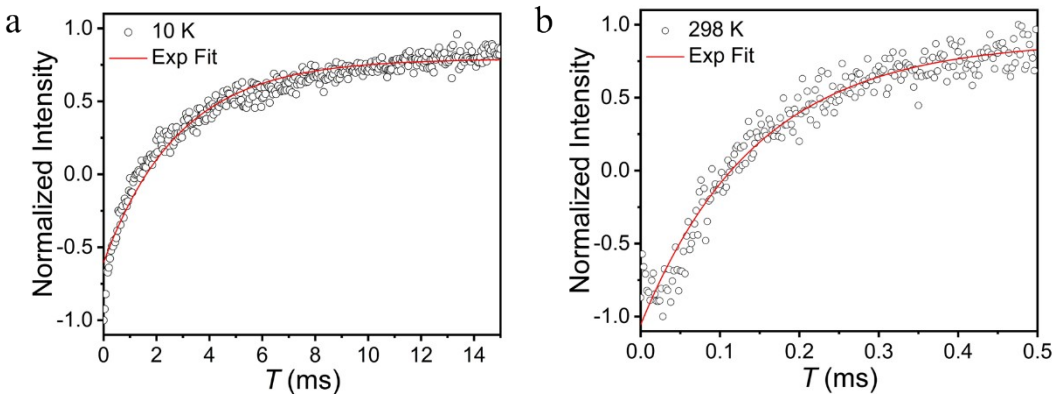

Figure S3 T_1 data measured at 10 K and 298K at 3456 G for 5 powder.

Table S1. T_1 data between 10-250 K of 3 powder at 3456 G.

T / K	3-T_1 / ms
10	3.005
20	2.19
40	1.042
60	0.787
80	0.51
100	0.322
150	0.202
200	0.132
250	0.06
298	0.04

Table S2. T_1 data of 5 powder at 10 K and 3456 G.

T / K	5-T_1 / ms
10	2.847
298	0.146

SI 3: T_m measurement of 3 and 5

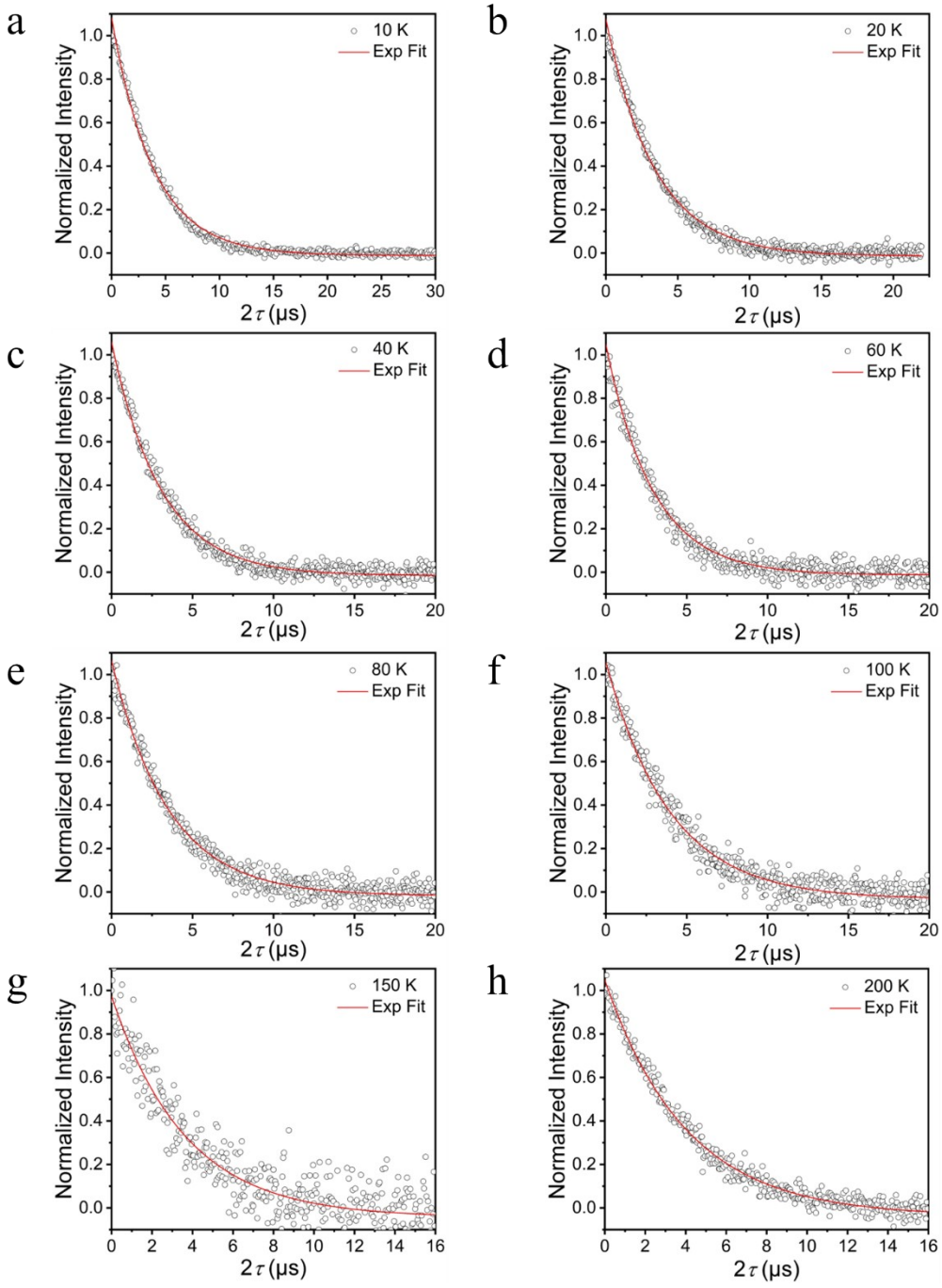

Figure S4 T_m data (black point) measured at different temperatures at 3456 G and individual exponential fitting curves (red line) for 3 powder. The shots per point for Figure S4 h (200 K) are twice as many as those used for Figure S4 a–g (from 10 to 150 K).

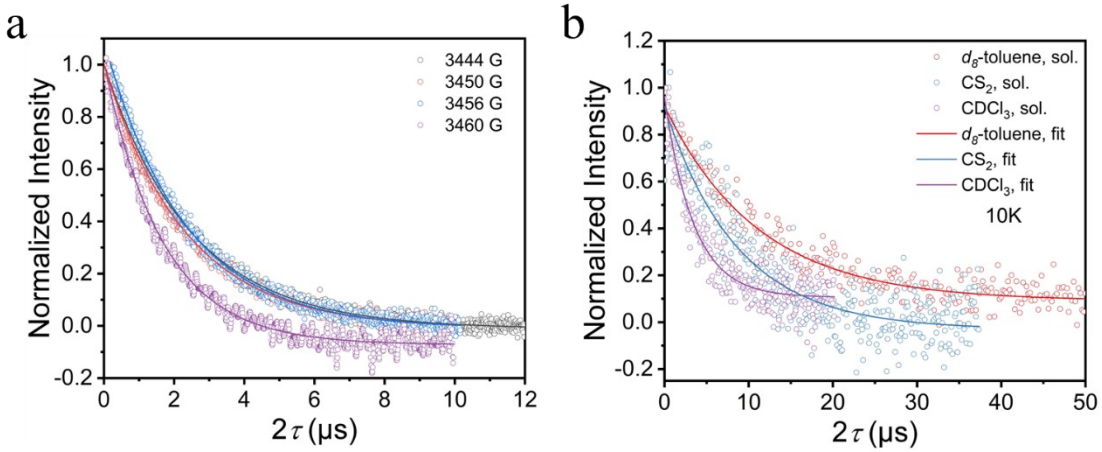

Figure S5 (a) T_m data (point) measured in different fields at 298 K and individual exponential fitting curves (line) for 3 powder. (b) T_m data (point) measured in different solutions at 10 K at 3456 G and individual exponential fitting curves (line) for 3.

Table S3. T_m data between 10-298 K of 3 powder at 3456 G.

T / K	3-T_m /μs
10	3.852
20	3.399
40	3.06
60	2.903
80	3.504
100	3.968
150	3.639
200	4.01
298	2.282

Table S4. T_m data of 3 in different fields at 298 K.

Field	3-T_m /μs
3444	2.456
3450	2.311
3456	2.282
3460	1.666

Table S5. T_m data of 3 in different solutions at 10 K and 3456 G.

Solvent	3-T_m /μs
d_8-toluene	11.156
CS_2	8.688
$CDCl_3$	3.469

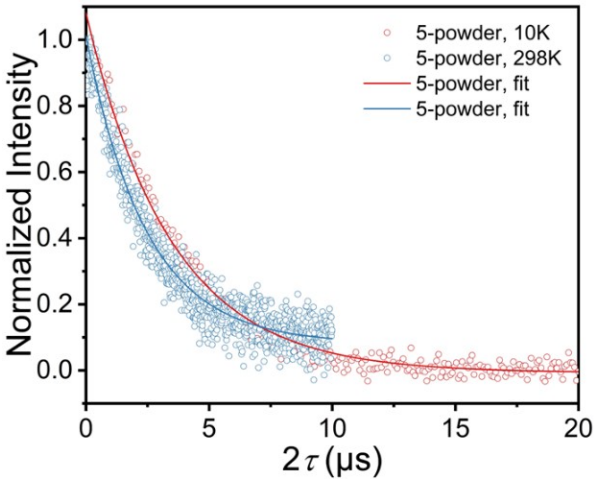

Figure S6 T_m data (point) measured at 10 K and 298 K at 3456 G and individual exponential fitting curves (line) for 5 powder.

Table S5. T_m data of 5 powder at 10K and 298 K at 3456 G.

T / K	5-T_m /μs
10	3.448
298	2.444

SI 4: T_m measurement of 3 and 5 powder with CPMG dynamic decoupling

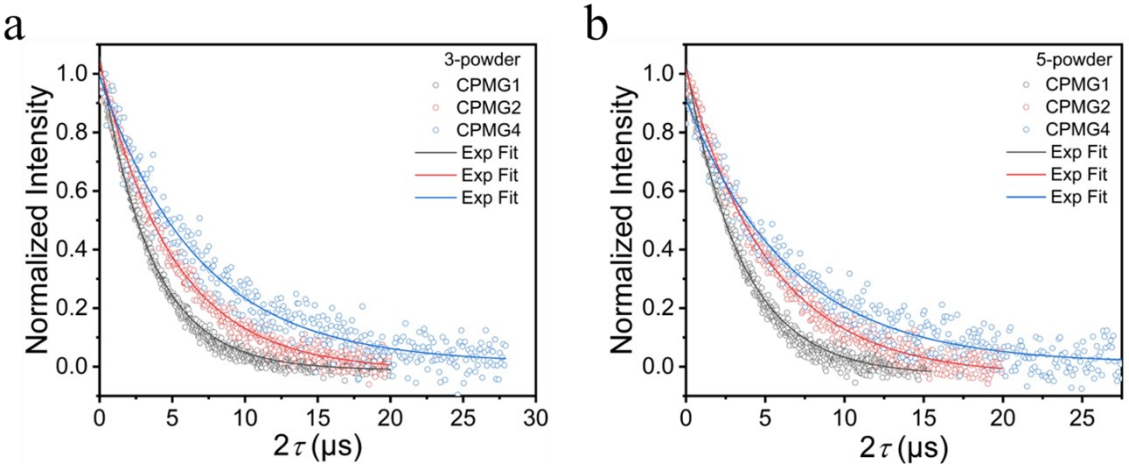

Figure S7 CPMG data (point) measured at 10 K at 3456 G and individual exponential fitting curves (line) for (a) 3 powder. (b) 5 powder.

Table S6. CPMG data of 3 and 5 powder at 10 K and 3456 G.

Inversion pulse number	3-T_m /μs	5-T_m /μs
1	3.487	3.5
2	5.034	5.318
4	6.732	6.49

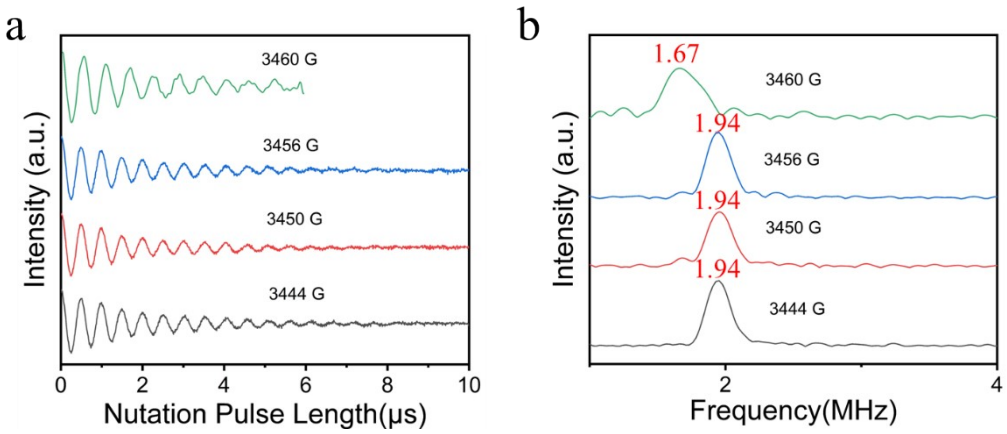

SI 5: Rabi oscillations of 3 and 5

Figure S8 (a) Rabi oscillations of the 3 powder measured at different fields at 298 K, 18 dB. (b) FFT of Rabi oscillations measured at different fields at 298 K, 18 dB.

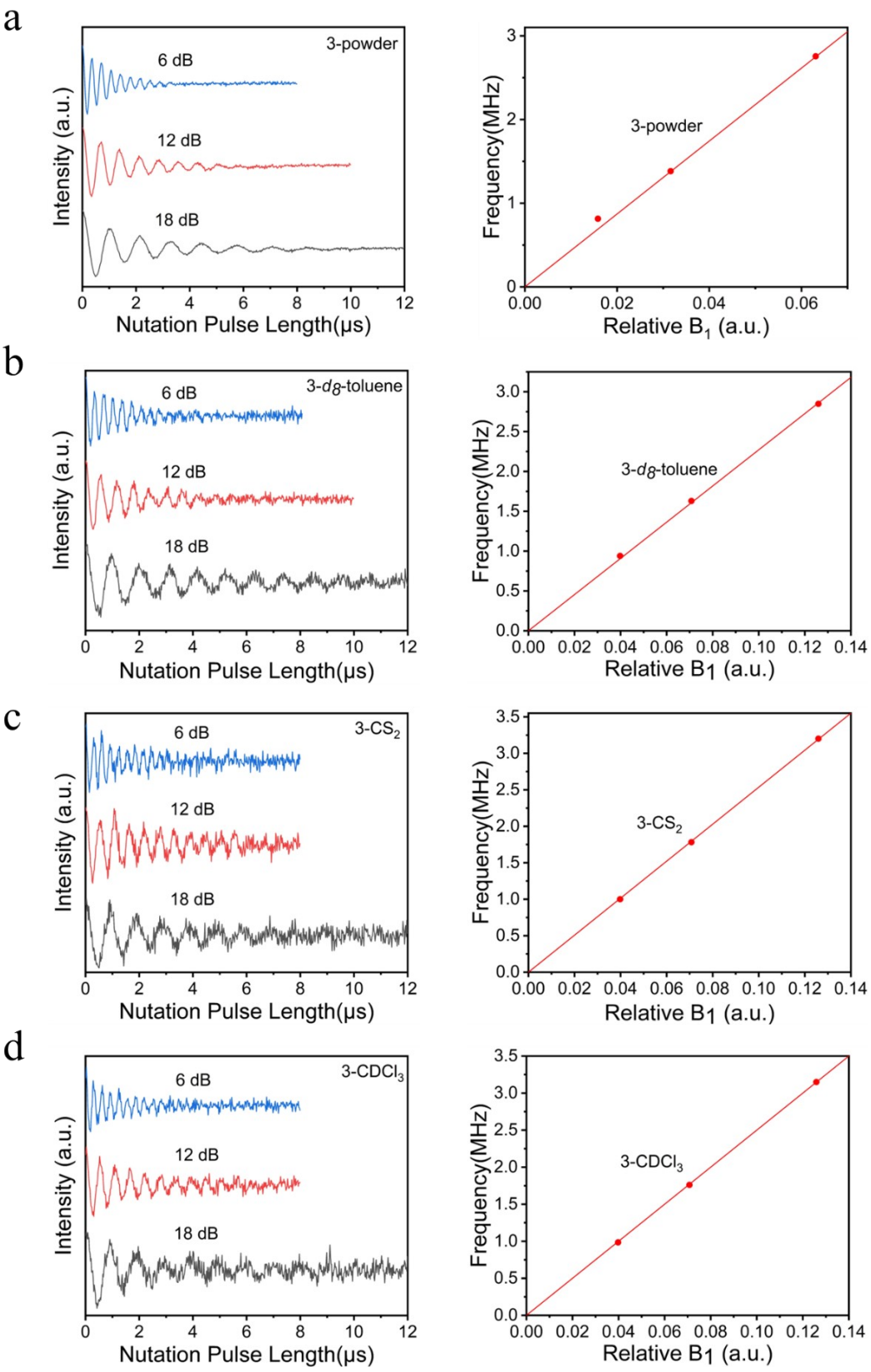

Figure S9 Rabi oscillations of (a) 3 powder, (b) 3 in d_8-toluene, (c) 3 in CS_2 and (d) 3 in $CDCl_3$ frozen solutions at 10 K and 3456 G for different pulse powers. The Rabi frequencies f_{Rabi} exhibit a linear relationship with the microwave B_1 field.

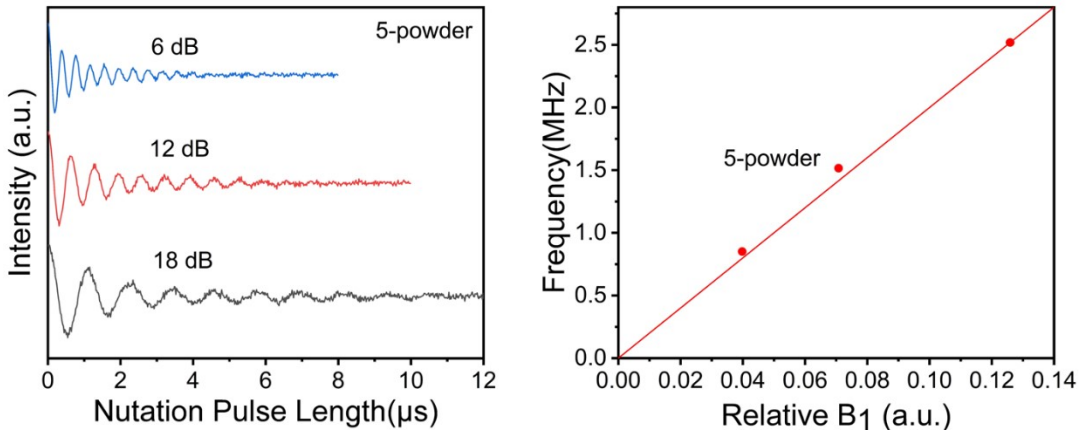

Figure S10 Rabi oscillations of 5 powder at 10 K and 3456 G for different pulse powers. The Rabi frequencies f_{Rabi} exhibit a linear relationship with the microwave B_1 field.